


## A structural module in RNase P expands the variety of RNA kinks

Mélanie Meyer, Eric Westhof & Benoît Masquida


To cite this article: Mélanie Meyer, Eric Westhof & Benoît Masquida (2012) A structural module in RNase P expands the variety of RNA kinks, RNA Biology, 9:3, 254-260, DOI: [10.4161/rna.19434](https://doi.org/10.4161/rna.19434)


To link to this article: <http://dx.doi.org/10.4161/rna.19434>



 View supplementary material 

 Published online: 01 Mar 2012.

 Submit your article to this journal 

 Article views: 126

 View related articles 

 Citing articles: 6 View citing articles 

# A structural module in RNase P expands the variety of RNA kinks

Mélanie Meyer, Eric Westhof and Benoît Masquida\*

Architecture et Réactivité de l'ARN, Université de Strasbourg, IBMC, CNRS; Strasbourg, France

**Keywords:** kink-turn, RNase P, RNA structure, RNA motif, RNA module, structural alignment

RNA structures are built from recurrent modules that can be identified by structural and comparative sequence analysis. In order to assemble sets of helices in compact architectures, modules that introduce bends and kinks are necessary. Among such modules, kink-turns form an important family that presents sequence and structural characteristics. Here, we describe an internal loop in the bacterial type A RNase P RNA that sets helices bound at the junctions exactly in the same relative positions as in kink-turns but without the structural signatures typical of kink-turns. Our work suggests that identifying a structural module in a subset of RNA sequences constitutes a strategy to identify distinct sequential motifs sharing common structural characteristics.

## Introduction

It is now well accepted that RNA structures are formed by the assembly of specific building blocks and that, among those, the A-form helix is the most represented. Standard Watson-Crick helices are separated by structural modules that organize the different domains in the three-dimensional space and confer to the molecule interaction capacities within the same RNA or with other RNAs, proteins and ligands (see ref. 1 for review). Comparative sequence analysis and crystallographic structures of RNA modules embedded in large RNAs have permitted the development of several *ab initio* and homology modeling strategies.<sup>2–5</sup> The success of *ab initio* modeling strategies relies on the correct attribution of a sequence to a given structural module. To achieve this goal, knowing all the sequences subjected to the formation of specific module is important.

RNA modules display a limited number of covariation rules. They are generally more difficult to characterize in terms of sequence because they are often complicated (1) by sequence variations (insertions or deletions of bulges); (2) by the complex network of interactions maintaining their integrity; and (3) by their propensity to make long distance contacts with RNAs or proteins. Based on precise structural alignments of sequences, progress toward the identification of known modules has been made.<sup>6,7</sup> This applies to the kink-turn (k-turn) module which generally connects two helices by means of a G-A tandem preceded on one side by an average 3 nt bulge (Fig. 1) with almost no sequence restrictions except those that arise from the anchoring of proteins which is systematically observed for k-turns found in rRNAs.<sup>8,9</sup> The G-A tandem accepts sequence variations in some cases, but those are restricted to the G-A pair distal from the bulge.<sup>9</sup> The two framing A-form helices adopt a specific relative

orientation consisting of a  $-90^\circ$  kink and a roughly  $-180^\circ$  twist between the Watson-Crick base pairs contiguous to the non-Watson-Crick part of the module.

Here we report an RNA module fully distinct from all other modules kinking RNA that have been described to date.<sup>9</sup> It consists of an asymmetrical internal loop that orients the framing helices exactly as regular k-turns do. This module occurs in the crystal structure of the bacterial RNase P holoenzyme bound to its tRNA product<sup>10</sup> and is located in the P16-P17 domain. This motif is distinct from the putative k-turn that has been described in the P12 domain of the human RNase P RNA.<sup>11</sup> For these reasons, it was named the pk-turn (p stems from RNase P). With respect to kinking and twisting of the framing helices, the pk-turn presents the same architectural properties as k-turns, albeit with completely different base pairs and sequence requirements. If structural modules are defined as sets of ordered non-Watson-Crick pairs embedded within Watson-Crick pairs,<sup>7</sup> then the pk-turn could be viewed as a new module. However comparative sequence analysis shows that some RNase P sequences present a standard k-turn module at this specific place. Following this definition, the pk-turn increases the sequence diversity of the known kinking modules. This observation helps to understand how RNA modules are selected and evolve from a pool of sequences and comforts the view that module conservation throughout the phylogeny is not pre-required to prove the occurrence of a motif. On the opposite, the finding of a module in a narrow subset of the phylogenetic tree seems to point to regions where distinct modules sharing common structural characteristics intervene. This idea could be applied to interpret sequence alignment results, to refine computational search of RNA modules in sequence databases, to infer some of their functional aspects, and to improve molecular modeling strategies.

\*Correspondence to: Benoît Masquida; Email: b.masquida@ibmc-cnrs.unistra.fr  
Submitted: 12/14/11; Revised: 01/19/12; Accepted: 01/20/12  
<http://dx.doi.org/10.4161/rna.19434>

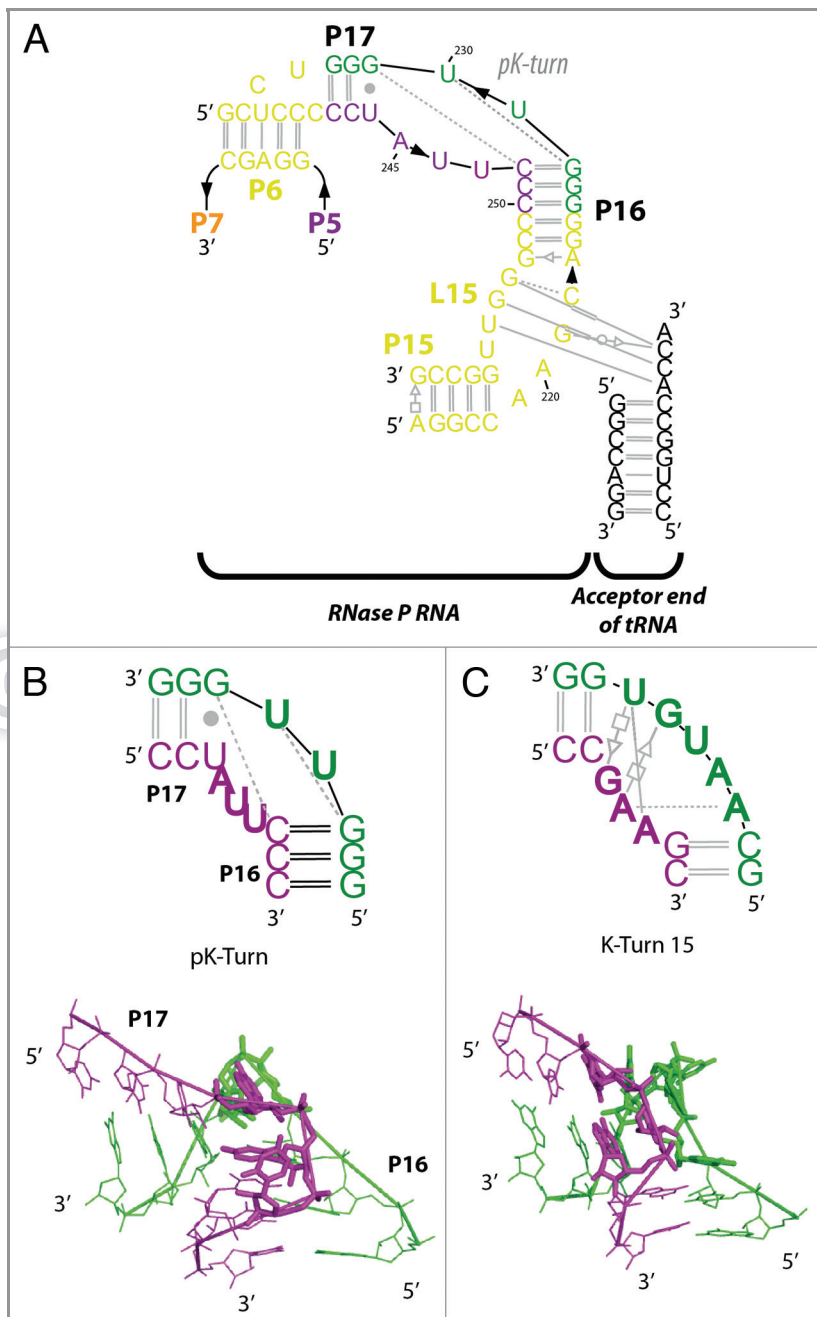


**Figure 1.** Secondary structure of the region comprising the pk-turn (A). Residue numbering is according to.<sup>10</sup> The scheme shows how the pk-turn is critical for the simultaneous correct presentation of the P6 pseudoknot and of the L15 loop that interacts with the acceptor end of the pre-tRNA substrate (black lettering). Comparative secondary and 3D structures of the pk-turn (B) and of the classical k-turn number 15<sup>6</sup> (C) from the *Haloarcula marismortui* 23S ribosomal crystal structure.<sup>33</sup> Residues unpaired or involved in non-canonical interactions are in bold face. The sequence motifs are completely distinct although they produce the same kink-turn between the bound helices. On the 3D panel (bottom), residues forming helices are drawn in thin lines and residues constituting the non-canonical motif are represented by sticks.

### Material and Methods

The pk-turn module was identified in the RNase P holoenzyme crystal structure<sup>10</sup> and superimposed with the k-turn-15<sup>6</sup> using all

backbone atoms from residues listed in Table S1. The *rmsd* and the translation-rotation matrices were calculated using lsqman.<sup>12</sup> 3D pictures were prepared using PyMOL<sup>13</sup> and Assemble.<sup>3</sup> All secondary structures from bacterial RNase P type A RNAs from the RNase P database<sup>14</sup> were checked and sorted according to their specific features (see **Supplemental Material**). A sequence alignment was derived using S2S.<sup>15</sup> The pk-turn candidate sequences were aligned to define a consensus using the program RNAalifold.<sup>16</sup> Sequences with extended bulges with respect to the reference *T.maritima* structure were considered as outliers and not considered in the consensus definition.

### Results

Early modeling studies<sup>17,18</sup> and the crystal structure of the naked bacterial type A RNase P RNA<sup>19</sup> have shown that a kink has to occur in the region of the RNase P RNA encompassing stems P15/P16/P17 responsible for the binding of the acceptor end of the pre-tRNA substrate. However, its precise location as well as its architecture have only been revealed by the recent crystal structure from the *Thermotoga maritima* RNase P ribozyme,<sup>10</sup> in which the addition of the tRNA to the holoenzyme contributes to the stabilization of this region. Despite its average resolution (3.8 Å), the crystal structure shows without ambiguity that the kink takes place at the internal loop separating P16 from P17. Close inspection of the kink shows that it is distinct from the known k-turns<sup>8,9</sup> in terms of sequence and base pair geometry of the internal loop. However, the relative positions and orientations of the framing helices are common to the standard k-turn module.

The formation of the RNase P P16/P17 kink results from the flexibility of the two strands composing the internal loop. One U residue of each strand bulges out (U229 and U247) while U246 is oriented within the helical stack and could form a *trans* Watson-Crick base pair with G228 if the latter were not already involved in pairing with C248 (Fig. 1). The only purine of the motif (A245) provides stacking continuity by capping P17. The absence of G residues obviously departs from the characteristic k-turn G-A pair directly following the bulge. Most importantly, P16 and P17, the stems bound to the RNase P

kink-turn, superimpose very well with the stems bound to a regular k-turn (*rmsd* of 1.5 Å; Fig. 2), as is the case for the superimpositions performed between different k-turns (reported in ref. 8).

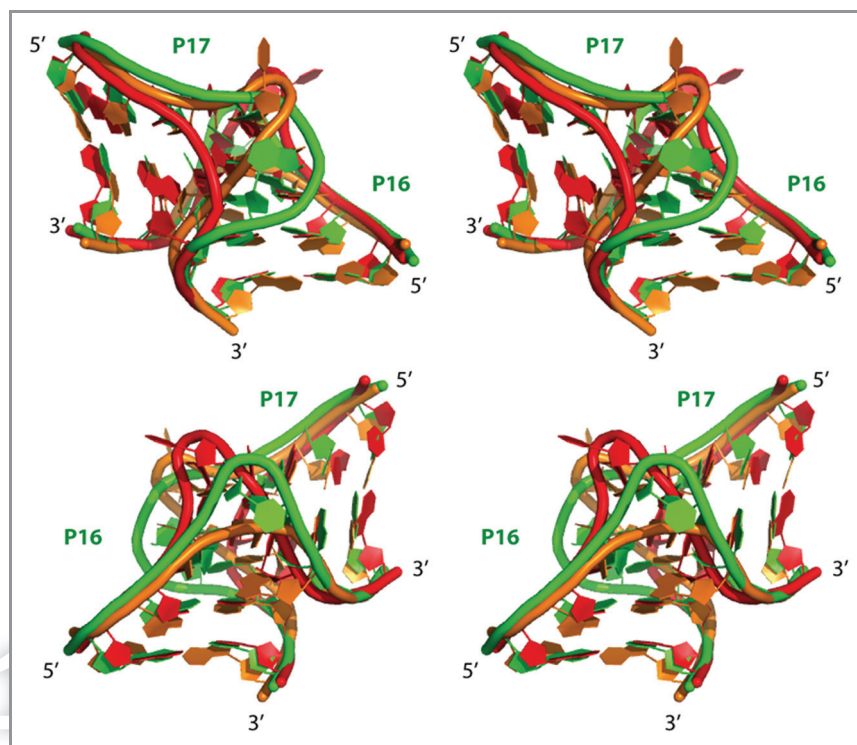


**Figure 2.** Wall-eye stereo view of the superimposition between the pk-turn (green ribbon, residues 235–242 and 251–259; PDB ID code 3OK7) and k-turn 15 (kt-15, residues 245–249 and 259–265; PDB ID code 1S72) in two opposite orientations (orange and red ribbons). Superimposition of the backbone atoms of the two Watson-Crick base-pairs of the helices bound to each motif were performed using *Isqman*.<sup>12</sup> The view on the lower panel is rotated 180° toward the view on the upper panel. *Rmsd* values and residues used in their determination are listed in Table S1.

Analysis of 295 secondary structures representative of the bacterial phylogeny (secondary structures from the RNase P database<sup>14</sup>) reinforces this observation (Table 1). A significant portion of bacterial type A RNase P RNA seemingly carries at this position a motif that fully respects the structural constraints characteristic of a regular k-turn module in several organisms (*Deinococcus*, *Thermus*, high G + C Gram<sup>+</sup>, *Mycobacterium tuberculosis*). Interestingly, both positions of the 3 nt bulge with respect to the G residues from the G-A tandem are observed in the sequences bearing a k-turn (Fig. 3, upper panel, and Fig. 4). In RNase P, the most abundant k-turns have their G-A tandem rooted in P17 (Table 1). Inspection of the secondary structures also shows that three-way junctions (3WJ, in *Chlamydia*, *Clostridium sporogenes*,  $\alpha$  purple bacteria) and four-way junctions (4WJ, in *Bacteroides* and *Planctomycetes*), occur between P16 and P17 (Fig. 3, lower panel).

Among internal loops, k-turns are represented in ~20% and pk-turns in 5% of the considered structural alignments. Hence, those modules do not represent the majority of the internal loops observed in this region. Roughly 40% of the aligned sequences exhibit a 2 to 5 nt bulge in J16/17 not evenly scattered within phyla but mostly occurring in  $\gamma$  purple bacteria and cyanobacteria. A couple of sequences with a bulge in J17/16 is also observed (*Propioniferax innocua*, *Aeromicrobium erythreum* and *fastidiosum*). It is difficult to infer the structure of these bulges directly from the alignments. Nonetheless, it seems very likely that a kink should also occur at this place since the secondary structure from the

*Thermotoga maritima* RNase P enzyme is very similar to the one from  $\gamma$  purple bacteria and cyanobacteria. Moreover, P16 and P17 are systematically longer in the latter phyla (6 and 5 bp or 6 and 3 bp, respectively) than in *Thermotogales* (5 and 3 bp). This observation could indicate that fraying of some base pairs may take place to facilitate the proper conformation.

A structural alignment restricted to internal loops (Fig. 4) illustrates how the four main families of modules could interchange and play equivalent roles. The k-turn modules are split between two families, having the bulge either in J16/17 (KT1) or in J17/16 (KT2). KT1 largely dominates (Table 1). In these two situations, the G-A tandem extends P17 or P16, respectively (Fig. 3). A similar situation is observed for the pk-turn module. The majority of the observed pk-turns (11 in 15) is composed of an asymmetrical internal loop with a J17/16 strand longer than the J16/17 one while fewer sequences have the opposite configuration (4 in 15, Table 1). The *Borrelia burgorferi* motif (Fig. 3) certainly represents an alternative sequence to the *T. maritima* pk-turn since the sequence of the closely related *Borrelia hermsii* is indeed very close to it (Fig. 5A). Some *Prochlorococcus* representatives seem to represent an intermediate stage between the *Thermotoga* and *Borrelia* pk-turn motifs. It is important to note that the kink between the helices allows easy accommodation of slightly longer bulges in J16/17 and J17/16 explaining why some pk-turns present one or two nucleotides insertions. The sequences from these three genus were used to produce a consensus of the pk-turn motif (Fig. 5B). On the opposite,



**Table 1.** Classification and distribution by phylum of motifs occurring in the secondary structures of the RNase P RNA P16-P17 region

	Purple Bacteria						Gram+G+C		Cyano	Bacte	Spiro	Chlam	Plancto	Green S	Green NS	Deino	Therm	UA	Total
	$\alpha$	$\beta$	$\gamma$	$\delta$	$\epsilon$	U	High	Low											
3WJ1	15	3	10	1	-	1	6	-	-	1	-	-	6	2	-	-	-	12	57
3WJ2	-	-	-	-	-	-	-	1	-	2	-	24	-	-	-	-	-	5	32
K-T1	-	9	1	2	-	1	38	-	-	-	-	-	-	3	-	-	2	56	
K-T2	-	-	-	-	-	-	-	-	-	-	-	1	-	-	3	-	-	4	
pKT1	-	-	-	-	-	-	-	-	5	-	2	-	-	-	-	2	2	11	
pKT2	-	-	-	-	-	-	-	-	4	-	-	-	-	-	-	-	-	4	
npKT1	7	-	65	-	-	5	-	5	22	1	2	1	-	-	-	-	8	116	
npKT2	-	-	-	1	-	-	3	-	-	-	2	-	-	-	-	-	-	6	
4WJ	-	-	-	-	-	-	-	-	-	1	-	-	1	-	-	-	-	4	
DP16	-	-	-	-	3	-	-	-	-	-	-	-	-	-	-	-	2	5	
total	22	12	76	4	3	7	47	6	31	5	6	25	8	2	3	3	2	33	295

3WJ1, Three-way junction with additional hairpin inserted between in J16/17; 3WJ2, Three-way junction with additional hairpin inserted between in J17/16; KT1, k-turn with GA tandem anchored in P17; KT2, k-turn with GA tandem anchored in P16; pKT1, pk-turn found in the *Thermotoga maritima* RNase P RNA crystal structure with J16/17 shorter than J17/16 or inserted in opposite orientation (pKT2); npKT1, Motifs expected to form a k-turn based on a 3 to 4 nt bulge in J16/17 or J17/16 (npKT2); 4WJ, Four-way junction with either two hairpins inserted in J17/16 or one hairpin in each junction between P16 and P17;  $\Delta$ P16, Case specific to the  $\epsilon$  subdivision of purple bacteria in which P16 is deleted resulting in a large L15 loop directly connected to P17. U, purple bacteria of uncertain affiliation; Cyano, cyanobacteria; Bacte, Bacteroides; Spiro, Spirochaetes; Plancto, Planctomycetes; Green S, green sulfur bacteria; Green NS, green non-sulfur bacteria; Deino, Deinococci; Therm, Thermotogales; UA, bacteria of uncertain affiliation.

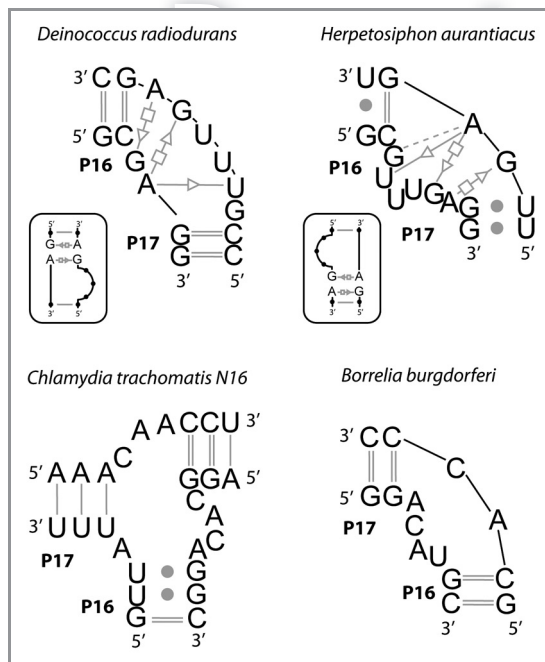


**Figure 3.** Examples of secondary structures of different motifs intervening at the P16-P17 junction in the bacterial type A RNase P RNA. *D. radiodurans* and *H. aurantiacus* RNase P RNAs show the presence of a k-turn in place of the pk-turn motif. Interestingly these k-turns are inserted in opposite orientations (see insets corresponding to each secondary structure). The relative orientations of P16 and P17 seems to be conserved also by means of a 3-way junction (*C. trachomatis*) or by other motifs of adopting a structure presumably close to the pk-turn (*B. burgdorferi*).

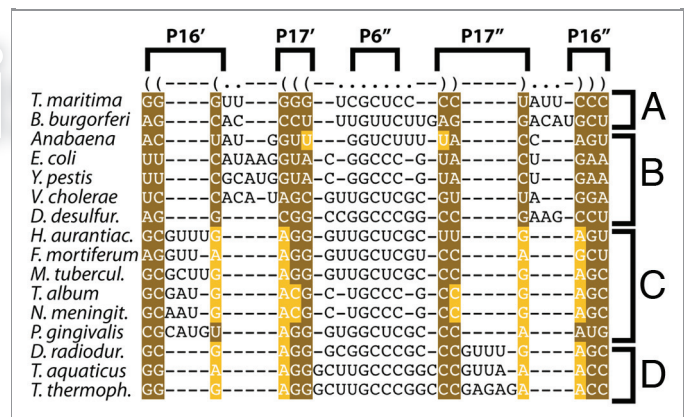


**Figure 4.** Alignment of a set of sequences of type A RNase P RNAs representative of the bacterial phylogeny. Sequences were gathered from the RNase P database.<sup>14</sup> Brown boxes indicate Watson-Crick conservation of base pairs forming P16 and P17 stems. Orange residues within these boxes indicate non-isosteric *cis* WW base pairs (Anabaena, *T. album*, *N. meningitidis*) or non-canonical *trans* SH G-A pairs (sequences in groups C and D) according to the LW base pair classification.<sup>34</sup> Sequences are sorted according to the type of motif contained in the loop connecting P16 to P17. (A) pk-turn, (B) kink-turns with unknown structures, (C) k-turns with the bulge upstream of the G-A tandem in the junction between P16 and P17 (J16/17), (D) k-turns in orientation opposite to (C), with the bulge upstream of the G-A tandem in J17/16. Purple bacteria: *Neisseria meningitidis*, *Escherichia coli*, *Vibrio cholerae*, *Yersinia pestis*, *Desulfovibrio desulfuricans*; Gram<sup>+</sup> bacteria: *Mycobacterium tuberculosis*; cyanobacteria: *Anabaena*; Bacteroides and relatives: *Porphyromonas gingivalis*; Spirochaetes: *Borrelia burgdorferi*; green non-sulfur bacteria: *Herpetosiphon aurantiacus*; Deinococcus and relatives: *Deinococcus radiodurans*, *Thermus thermophilus*, *Thermus aquaticus*; Thermotogales: *Thermotoga maritima*; bacteria of uncertain affiliation: *Fusobacterium mortiferum*.

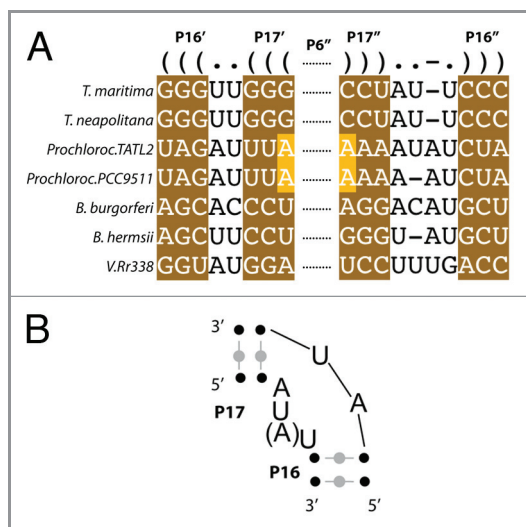


**Figure 5.** Alignment of a subset of pk-turn candidate sequences in the RNase P P16/P17 region. (A) The 7 sequences shown are representative of the three genus displaying the pk-turn. Sequences with extended bulges were removed and the same number of sequences for each genus was taken in order to avoid increasing the impact of outliers as described in.<sup>16</sup> Sequences not used in **Figure 4** include *Thermotoga neapolitana*, *Prochlorococcus TATL2*, *Prochlorococcus PCC9511*, *Borrelia hermsii*, *Volunteer Rr338* (Seq ID: AF296062). (B) Consensus secondary structure derived from the alignment using the program RNAalifold.<sup>16</sup> The A residue in parenthesis corresponds to an insertion observed in the *Prochlorococcus* and *Borrelia* genus.

hypothetical non-*Thermotoga maritima* pk-turns (npk-turn) are characterized by a 2–5 nt bulge in J16/17 structurally closer to k-turns with the bulge in J16/17. Thus, all these sequence motifs are expected to form genuine kink-turns accommodating the formation of the P6 pseudoknot together with the interaction with the pre-tRNA substrate. However, unlike for the pk-turn, the absence of a npk-turn crystal structure prevents to assess whether npk-turns promote folding of the P16/P17 region by means of positioning the stems as the pk-turn does. Along the same line of idea, it is reasonable to hypothesize that the 3WJ and 4WJ should also preserve the relative orientation of P16 and P17. Rare exceptions to this general trend are seen in organisms (ε purple bacteria, *Campylobacter jejuni* and *Helicobacter pylori*) with an RNase P RNA in which P16 is seemingly absent resulting in a large L15 loop directly connected to P17. In these cases, it is likely that the extended L15 may form a kink-turn as in RNase P RNAs from other phylogenetic groups, although, no evidence can be presented.

## Discussion

The impressive molecular resemblance between the pk-turn and k-turns constitutes a strong piece of evidence that RNase P RNAs with a P16/P17 sequence containing the k-turn constraints indeed fold as such. This study thus shows how the pk-turn replace k-turns to play an equivalent structural role in an homologous region of the RNase P RNAs. This provides a convincing illustration of how evolution selects different RNA

sequences to promote the formation of equivalent modules,<sup>1</sup> in this case, a k-turn or k-turn-like sequential motifs to favor the presentation of the pre-tRNA substrate to the RNase P enzyme. Moreover, the k-turn strands can be exchanged without affecting the relative orientation of P16 and P17 (KT1 or KT2, **Table 1**). Interestingly, the strands composing a loop E motif in the GOLD RNA<sup>20</sup> are also found exchanged in a sequence subset. The exchange between the k-turn strands suggests that the recognition of the pre-tRNA substrate together with the formation of the P6 pseudoknot establish the main selection pressures that drive the evolution of the sequence in the junction between P16 and P17. This conclusion could lead to a strategy to elucidate whether given RNA modules interact or not with proteins. Most k-turns indeed interact with proteins to form asymmetric complexes as between the 15.5 kD protein and the snRNA U4 k-turn<sup>21</sup> or between k-turns found in rRNAs and their cognate proteins.<sup>8</sup> In these cases, inverting the k-turn is equivalent to swapping the bulge and the G-A tandem from one stem to the other and thus to change the orientation of the bound protein. We can then conclude from the observation that the P16/P17 junction harbors k-turns in both orientations that it does not require any cognate protein during catalysis since it would result in two different binding modes for a candidate protein across the phylogeny. Developing analysis methods to search for inverted motifs within homologs would thus help systematically finding domains that may favor protein binding.

It is worth noting that the *Thermotoga maritima* lysine riboswitch also presents a kink-like module between stem P2a and loop L2 that is replaced by a regular k-turn in other lysine riboswitches.<sup>22</sup> However, superimposition of the considered P2a-L2 motif with kt-7 from 16S rRNA or with the kink from the P4P6 domain from the Tetrahymena group I intron<sup>23</sup> fails to show a straightforward structural relationship between those three motifs.<sup>24</sup> The lysine riboswitch P2a-L2 motif takes place in a context very different from the k-turn since the L2 loop forms a pseudoknot with L3 and thus cannot be considered as an internal loop per se. The resulting different topology in which this motif ascribes itself raises the question of what precise structure would adopt the L2 k-turn sequence. Along the same line of idea, k-turn forming sequences can also fold in a reverse orientation<sup>25</sup> as seen in the P9 domain of the Azoarcus group I ribozyme crystal structure.<sup>26</sup> Yet, the structural context forces it to adopt a different base-pairing scheme to support the formation of the critical tertiary interaction between the L9 tetraloop and its receptor located in P5. Grafting of a consensus k-turn sequence in the P9 domain does not modify the overall fold as proven by the crystal structure of an Azoarcus group I ribozyme mutant.<sup>27</sup> If k-turns and most probably other RNA modules can be forced to adopt other conformations, it is thus likely that the opposite situation may also be true. Sequences not respecting the consensus for a k-turn may be forced by the structural context to adopt a k-turn conformation. The energetic constraints imposed by the whole RNA architecture and contacts stabilizing the crystal packing may thus force proper folding of a given module. This idea is supported by a recent experimental study on the SAM-I riboswitch in which mutants of the k-turn motif which prevent

correct folding in isolation have no effect in the context of the full length riboswitch.<sup>28</sup>

As mentioned above, crystal structures of the P16/P17 region based on 2–5 nt bulges (npk-turn) are missing. Nevertheless, modeling of these bulges shows that fraying of at least one base pair from either P16 or P17 is necessary to force the stems to adopt a conformation favoring the formation of contacts between the shallow grooves of the stems characteristic of k-turns (data not shown). Without fraying, the kink serves to move away the two bound stems so that the deep grooves face each other as observed in two recent crystal structures.<sup>29,30</sup> Fraying actually occurs in the *Thermotoga maritima* RNase P RNA<sup>10</sup> in which nucleotides involved in the first base pair of P17 do not interact in the crystal structure in contradiction with the initial secondary structure. Rather these residues help mediate smooth connections between P16 and P17 in order to facilitate the pk-turn fold. These conclusions bring the idea that the overall architecture of the RNase P RNA may energetically force the folding of the P16/P17 domain to form a kink-turn explaining why this region accepts a high level of sequence variations. The consensus deduced in this study (Fig. 5B) may now be used to identify new occurrences of the pk-turn in other RNAs using a variety of strategies.<sup>7,31</sup>

Other motifs (2–5 nt bulges, 3WJ and 4WJ) found within the secondary structure data set should also be instrumental in precisely orienting P16 and P17 so that they roughly form a 90° angle and their shallow grooves interact. The 2–5 nt bulge in J16/17 may represent a family of motifs aiming at inserting a local energetic instability that will appropriately respond to P6 folding by acquiring a kinked conformation. 3WJ are known for mediating fairly precise angles between their stems.<sup>32</sup> One of the three families of 3WJ (family A) specifically fulfills both the angle between the helical stack and the third helix and the contacts between the shallow grooves.

It has been noted that k-turns are not always conserved in all phylogenetic groups for rRNAs.<sup>6</sup> The example found in the RNase P holoenzyme crystal structure describes how k-turns are replaced in certain branches of the phylogenetic tree by other structurally equivalent modules. The definition of k-turns and RNA modules in general is based on the network of specific interactions taking place between nucleotides and results in a consensus sequence. Their structural features like the relative positions and orientations of connected helices are usually considered as facilitated by the interaction network. Here, we illustrate how defining a motif based on its structural features offers an original strategy to identify new interaction networks that offset the consensus and result in the same overall relative positions and orientations of helices. Thorough conservation of a module throughout the phylogeny is thus not required to conclude for its existence. On the opposite, the presence of a given motif even in a small subset of sequences may contribute to identify other motifs that are not homologous in sequence but may share common structural features.

#### Disclosure of Potential Conflicts of Interest

No potential conflicts of interest were disclosed.

#### Acknowledgments

This work was supported by the University of Strasbourg (PhD grant CDOC 2010\_117 to M.M.), the Centre National de la Recherche Scientifique and the Université de Strasbourg (to B.M. and E.W.). We thank Pascal Auffinger for helpful discussions and critical reading of the manuscript.

#### Supplemental Materials

Supplemental materials may be downloaded here:

[www.landesbioscience.com/journals/rnabiology/article/19434](http://www.landesbioscience.com/journals/rnabiology/article/19434)

#### References

- Masquida B, Beckert B, Jossinet F. Exploring RNA structure by integrative molecular modelling. *N Biotechnol* 2010; 27:170-83; PMID:20206310; <http://dx.doi.org/10.1016/j.nbt.2010.02.022>
- Das R, Karanicolas J, Baker D. Atomic accuracy in predicting and designing noncanonical RNA structure. *Nat Methods* 2010; 7:291-4; PMID:20190761; <http://dx.doi.org/10.1038/nmeth.1433>
- Jossinet F, Ludwig TE, Westhof E. Assemble: an interactive graphical tool to analyze and build RNA architectures at the 2D and 3D levels. *Bioinformatics* 2010; 26:2057-9; PMID:20562414; <http://dx.doi.org/10.1093/bioinformatics/btq321>
- Rother M, Rother K, Puton T, Bujnicki JM. ModeRNA: a tool for comparative modeling of RNA 3D structure. *Nucleic Acids Res* 2011; 39:4007-22; PMID:21300639; <http://dx.doi.org/10.1093/nar/gkq1320>
- Sijenyi F, Saro P, Ouyang Z, Damm-Ganamet K, Wood M, Jiang J, et al. The RNA Folding Problems: Different levels of RNA Structure Prediction. In: Leontis N, Westhof E, eds. *RNA 3D Structure Analysis and Prediction*: Springer, 2011.
- Lescoute A, Leontis NB, Massire C, Westhof E. Recurrent structural RNA motifs, Isostericity Matrices and sequence alignments. *Nucleic Acids Res* 2005; 33:2395-409; PMID:15860776; <http://dx.doi.org/10.1093/nar/gki535>
- Cruz JA, Westhof E. Sequence-based identification of 3D structural modules in RNA with RMDetect. *Nat Methods* 2011; 8:513-21; PMID:21552257; <http://dx.doi.org/10.1038/nmeth.1603>
- Klein DJ, Schmeing TM, Moore PB, Steitz TA. The kink-turn: a new RNA secondary structure motif. *EMBO J* 2001; 20:4214-21; PMID:11483524; <http://dx.doi.org/10.1093/emboj/20.15.4214>
- Schroeder KT, McPhee SA, Ouellet J, Lilley DM. A structural database for k-turn motifs in RNA. *RNA* 2010; 16:1463-8; PMID:20562215; <http://dx.doi.org/10.1261/rna.2207910>
- Reiter NJ, Osterman A, Torres-Larios A, Swinger KK, Pan T, Mondragón A. Structure of a bacterial ribonuclease P holoenzyme in complex with tRNA. *Nature* 2010; 468:784-9; PMID:21076397; <http://dx.doi.org/10.1038/nature09516>
- Rosenblad MA, López MD, Piccinelli P, Samuelsson T. Inventory and analysis of the protein subunits of the ribonucleases P and MRP provides further evidence of homology between the yeast and human enzymes. *Nucleic Acids Res* 2006; 34:5145-56; PMID:16998185; <http://dx.doi.org/10.1093/nar/gkl626>
- Kleywegt GJ, Jones TA. A super position. *CCP4/ESF-EACBM Newsletter on protein crystallography* 1994: 9-14.
- Schrodinger, LLC. The PyMOL Molecular Graphics System, Version 1.3r1. 2010.
- Brown JW. The Ribonuclease P Database. *Nucleic Acids Res* 1999; 27:314; PMID:9847214; <http://dx.doi.org/10.1093/nar/27.1.314>
- Jossinet F, Westhof E. Sequence to Structure (S2S): display, manipulate and interconnect RNA data from sequence to structure. *Bioinformatics* 2005; 21:3320-1; PMID:15905274; <http://dx.doi.org/10.1093/bioinformatics/bti504>
- Bernhart SH, Hofacker IL, Will S, Gruber AR, Stadler PF. RNAalifold: improved consensus structure prediction for RNA alignments. *BMC Bioinformatics* 2008; 9:474; PMID:19014431; <http://dx.doi.org/10.1186/1471-2105-9-474>
- Massire C, Jaeger L, Westhof E. Derivation of the three-dimensional architecture of bacterial ribonuclease P RNAs from comparative sequence analysis. *J Mol Biol* 1998; 279:773-93; PMID:9642060; <http://dx.doi.org/10.1006/jmbi.1998.1797>
- Harris ME, Kazantsev AV, Chen JL, Pace NR. Analysis of the tertiary structure of the ribonuclease P ribozyme-substrate complex by site-specific photoaffinity cross-linking. *RNA* 1997; 3:561-76; PMID:9174092
- Torres-Larios A, Swinger KK, Krasilnikov AS, Pan T, Mondragón A. Crystal structure of the RNA component of bacterial ribonuclease P. *Nature* 2005; 437:584-7; PMID:16113684; <http://dx.doi.org/10.1038/nature04074>

20. Weinberg Z, Perreault J, Meyer MM, Breaker RR. Exceptional structured noncoding RNAs revealed by bacterial metagenome analysis. *Nature* 2009; 462: 656-9; PMID:19956260; <http://dx.doi.org/10.1038/nature08586>
21. Vidovic I, Nottrott S, Hartmuth K, Lührmann R, Ficner R. Crystal structure of the spliceosomal 15.5kD protein bound to a U4 snRNA fragment. *Mol Cell* 2000; 6:1331-42; PMID:11163207; [http://dx.doi.org/10.1016/S1097-2765\(00\)00131-3](http://dx.doi.org/10.1016/S1097-2765(00)00131-3)
22. Garst AD, Héroux A, Rambo RP, Batey RT. Crystal structure of the lysine riboswitch regulatory mRNA element. *J Biol Chem* 2008; 283:22347-51; PMID:18593706; <http://dx.doi.org/10.1074/jbc.C800120200>
23. Cate JH, Gooding AR, Podell E, Zhou K, Golden BL, Kundrot CE, et al. Crystal structure of a group I ribozyme domain: principles of RNA packing. *Science* 1996; 273:1678-85; PMID:8781224; <http://dx.doi.org/10.1126/science.273.5282.1678>
24. Serganov A, Huang L, Patel DJ. Structural insights into amino acid binding and gene control by a lysine riboswitch. *Nature* 2008; 455:1263-7; PMID:18784651; <http://dx.doi.org/10.1038/nature07326>
25. Strobel SA, Adams PL, Stahley MR, Wang J. RNA kink turns to the left and to the right. *RNA* 2004; 10:1852-4; PMID:15547133; <http://dx.doi.org/10.1261/rna.7141504>
26. Adams PL, Stahley MR, Kosek AB, Wang J, Strobel SA. Crystal structure of a self-splicing group I intron with both exons. *Nature* 2004; 430:45-50; PMID:15175762; <http://dx.doi.org/10.1038/nature02642>
27. Antonioli AH, Cochrane JC, Lipchick SV, Strobel SA. Plasticity of the RNA kink turn structural motif. *RNA* 2010; 16:762-8; PMID:20145044; <http://dx.doi.org/10.1261/rna.1883810>
28. Schroeder KT, Daldrop P, Lilley DMJ. RNA tertiary interactions in a riboswitch stabilize the structure of a kink turn. *Structure* 2011; 19:1233-40; PMID:21893284; <http://dx.doi.org/10.1016/j.str.2011.07.003>
29. Dibrov SM, Johnston-Cox H, Weng YH, Hermann T. Functional architecture of HCV IRES domain II stabilized by divalent metal ions in the crystal and in solution. *Angew Chem Int Ed Engl* 2007; 46:226-9; PMID:17131443; <http://dx.doi.org/10.1002/anie.200603807>
30. Dibrov SM, McLean J, Parsons J, Hermann T. Self-assembling RNA square. *Proc Natl Acad Sci U S A* 2011; 108:6405-8; PMID:21464284; <http://dx.doi.org/10.1073/pnas.1017999108>
31. Bernhart SH, Hofacker IL. From consensus structure prediction to RNA gene finding. *Brief Funct Genomic Proteomic* 2009; 8:461-71; PMID:19833701; <http://dx.doi.org/10.1093/bfgp/elp043>
32. Lescoute A, Westhof E. Topology of three-way junctions in folded RNAs. *RNA* 2006; 12:83-93; PMID:16373494; <http://dx.doi.org/10.1261/ra.2208106>
33. Ban N, Nissen P, Hansen J, Moore PB, Steitz TA. The complete atomic structure of the large ribosomal subunit at 2.4 Å resolution. *Science* 2000; 289:905-20; PMID:10937989; <http://dx.doi.org/10.1126/science.289.5481.905>
34. Leontis NB, Westhof E. Geometric nomenclature and classification of RNA base pairs. *RNA* 2001; 7:499-512; PMID:11345429; <http://dx.doi.org/10.1017/S1355838201002515>

© 2012 Landes Bioscience.

Do not distribute.